Observations of the Low Earth Orbit Radiation Environment from Mir

P. Bühler[1], L. Desorgher[1], A. Zehnder[1], E. Daly[2], and L. Adams[2]

[1] Paul Scherrer Institute, CH–5232 Villigen PSI
[2] ESA/ESTEC, NL–2200 AG Noordwijk

Reference: *Radiation Measurements*, **26**, 917-921 (1996)

Abstract

Recent measurements of the high–energy charged particle environment with the Radiation Environment Monitor (REM) aboard of the Russian Mir space station are presented. Ionizing dose rates in a silicon detector have been measured with two shieldings. The dose is mainly accumulated in two distinct areas, the South Atlantic Anomaly (SAA) and the region of closest approach to the magnetic poles. Whereas the radiation in the South Atlantic Anomaly varied little during 1995, large changes of the daily absorbed doses in the polar regions are observed. A comparison of REM doses with the NASA AP–8 and AE–8 radiation models revealed major differences. AP–8 tends to underestimate the average REM doses, whereas AE–8 overestimates REM doses, and rather describes the worst case.

Introduction

The interaction of high energy charged particles with space vehicles can cause serious problems. Because these particles penetrate deep into the satellite and affect sensitive parts, such as electronics and scientific equipment, and also human beings in manned space stations, reliable prediction of expected radiation doses is of great importance for planning space missions.

For manned missions the Low Earth Orbit, LEO of the Russian Mir space station (altitude: 400 km, inclination: 52°) is of particular interest not only because Mir is actually the only permanently occupied station in orbit but also because the international space station is planned to be put in an equivalent orbit. The orbits of Space Shuttle flights vary in altitude and inclination and often cover parts of the Mir trajectory. Measurements of the radiation environment aboard Mir can thus be an important input for the future missions.

Instrument and Observations

In this paper we report on measurements of the high–energy particle environment with the Radiation Environment Monitor (REM) mounted outside the Mir space station. The observations cover the November 1994 to February 1996 period. During this period REM has been accumulating data for more than 50% of the available time. REM is planned to be operational aboard MIR until the end of 1996.

The REM instrument consists of two silicon detectors measuring energy loss spectra of charged particles (Bühler *et al.*, 1995). The ΔE spectra are accumulated for 32 seconds and binned into 16–channel histograms. Channel energies range from 10 keV (0.2 MeV cm^2/g, 0.1 minimum ionizing energy (MIP)) up to more than 100 MeV (2 GeV cm^2/g, 1000 MIP). The main aperture is defined by an aluminium cone with an opening angle of ±45°. The aperture of one detector (the "e–detector") is covered with a spherical dome of 0.7 mm aluminium. The aperture of the second detector (the "p–detector") is covered with 3 mm aluminium and an additional layer of 0.75 mm tantalum. For protons with an

energy of 50 MeV the additional tantalum layer is equivalent to approximately 2.9 mm of aluminium, and for electrons of 1 Mev the tantalum layer is equivalent to 3.6 mm. The aluminium equivalent shielding of the p–detector is thus about 5.9 and 6.6 mm for protons and electrons, respectively.

The dome thickness defines the lower cut–off energy, E_{th}, for particles able to penetrate into the detection volume. For electrons E_{th} is approximately 0.7 MeV in the e–detector and 2.6 MeV in the p–detector; for protons E_{th} is 10 MeV in the e–detector and 34 MeV in the p–detector. As the energy spectrum of the electrons in the encountered space environment decreases sharply above 0.7 MeV, an efficient suppression of electron detection in the p–detector compared to the e–detector can be expected.

The REM instrument is mounted on the outside of the Mir space station. It is fixed on railings encircling the Mir core module with the detector aperture directed perpendicular to the length axis of the station, towards the space.

Dose measurements

To quantify the measured radiation environment we calculated the dose deposit in the two detectors. For each 32–second accumulation we calculated the dose rate d with

$$d = \frac{1.6 \cdot 10^{-11}}{\rho \cdot V} \cdot \sum_{i=4}^{15} \overline{\Delta E_i} \cdot c_i \; [rad/sec] \tag{1}$$

where $\overline{\Delta E_i}$ is the mean energy deposit in keV per count in detector channel i, c_i is the count rate in detector channel i, ρ is the density of silicon in g/cm^3, and V the detector volume in cm^3. In order to calculate rads from Energy deposits we use the relation 1 rad = $6.24 \cdot 10^{10}$ MeV/kg. Channels 1 to 3 are not counted as they contain energies below 1 MIP (noise channels).

Spatial distribution

In Figure 1 contours of average deposited doses measured during August 1995 are plotted on a geographic map. The upper panel shows p–detector data and the lower panel e–detector data. Contour levels are given in mrad/min. Note that the inclination of the Mir orbit limits the observations to latitudes within $\pm 52°$.

Two regions of enhanced radiation can be distinguished, the South Atlantic Anomaly (SAA), a region centered on the east coast of South America, and the regions close to the earth magnetic poles (marked in Figure 1 with crosses), which, in the following, will be referred to as polar regions. Although the rest is not radiation free, its contribution to the total daily dose is below 0.1%.

The particles encountered are mainly protons and electrons trapped in the Van Allen radiation belts. The topology of the radiation regions is defined by the distribution of L–shell value and magnetic field strength at the orbit altitude. Large particle fluxes are encountered at minimum magnetic field and geomagnetic L–shell values between 1 and 2 in the SAA and between 3 and 6.5 in the polar regions.

SAA

The SAA is caused by the displacement of the earth's magnetic dipole axes relative to the earth's rotation axis. Due to this displacement, the earth's magnetic field has a local minimum in this region, that allows trapped particles of the inner radiation belt to penetrate to low altitudes. Because the energetic component of the inner radiation belt is mainly composed of protons, the radiation environment in the SAA is dominated by these particles. The dose rate measured in August 1995 in the center of the SAA is 3.6 mrad/min in the p–detector and 4.8 mrad/min in the e–detector. The difference between the two detectors is rather small, indicating that the additional p–detector shielding (about 5.9 mm aluminium) is not sufficient to significantly reduce the penetration of the environmental particles.

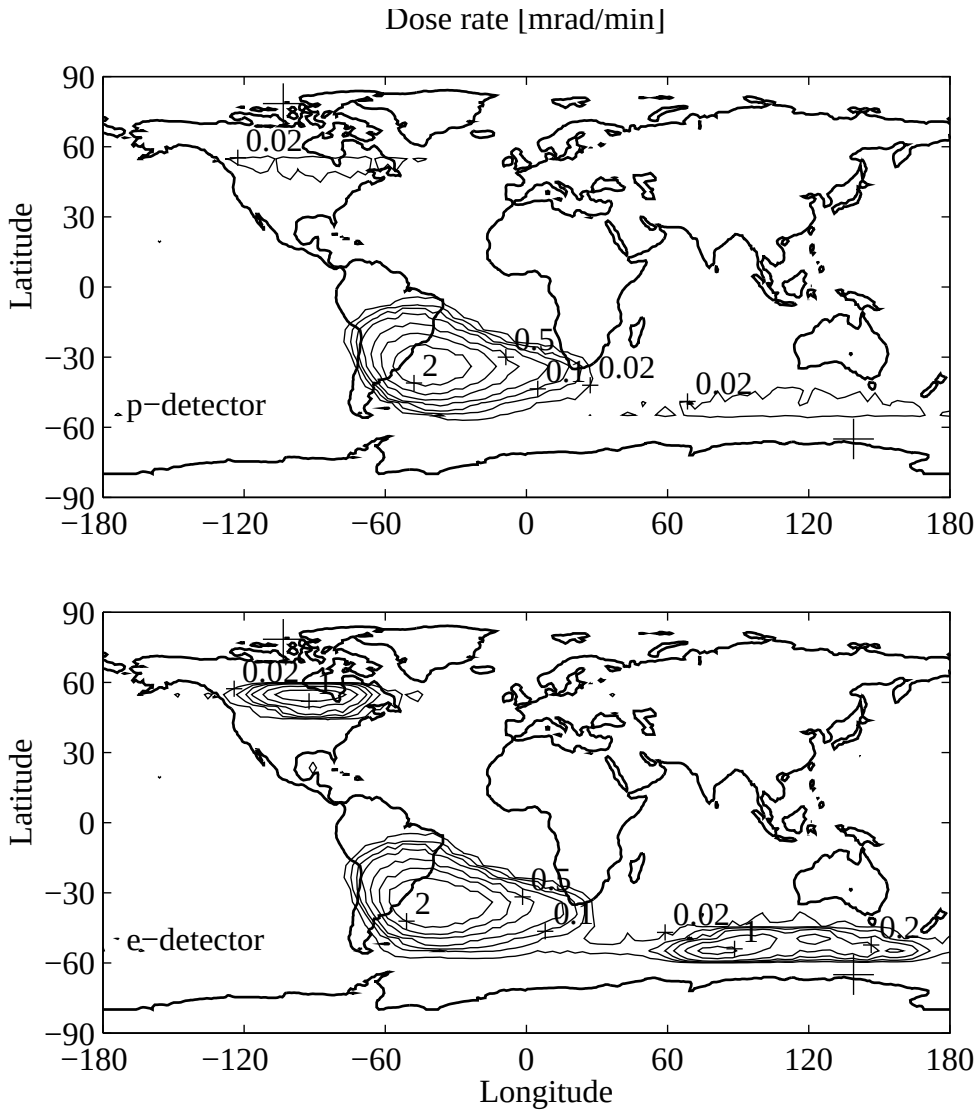

Figure 1: Average REM dose rates during August 1995. The contours show iso–dose rate levels measured in p–detector (upper panel) and e–detector (lower panel). The contour level values are 0.01, 0.02, 0.05, 0.1, 0.2, 0.5, 1, 2 mrad/min. The energy deposit in the polar regions is heavily reduced by the p–detector shielding, whereas the radiation in the SAA penetrates it.

Because the trapped particles are intimately linked with the magnetic field, the SAA is supposed to follow drifts of the earth magnetic field, particullarly the secular drift at a rate of approximately 0.3° per year.
To determine the actual position of the SAA we fit a gaussian to a cut through the dose map along the latitude of 35°. The determined maximum is located at -41.9° longitude. According to calculations using AP–8 MIN radiation model (Sawyer and Vette, 1976), the SAA in 1970 has been located at -35.4° longitude. In these 25 years the SAA has drifted west by 6.5°, representing an annual drift rate of approximately 0.26°. This value is in reasonable agreement with results found with measurements aboard Space Shuttle flights (Konradi *et al.*, 1994) and also with the secular drift rate of the geomagnetic field.

Polar regions
The particles encountered in the polar regions are outer belt electrons with equatorial pitch angles small enough to reach low altitudes at high magnetic latitudes. In August 1995 we find a maximum dose of 0.04 mrad/min in the p–detector and 1.6 mrad/min in the e–detector. The difference between the two detectors is large, indicating that the shielding of the p–detector is an effective protection against high–energy electrons.

Temporal variations

In this section we investigate temporal variations of the SAA and polar region average daily doses. The SAA and polar regions are therefore defined to be the rectangular regions enclosed by the following limits:

$$\begin{array}{ll} \text{SAA:} & -80^\circ \leq \text{longitude} \leq 40^\circ, \text{ latitude} \leq 0^\circ \\ \text{polar regions:} & -40^\circ \leq \text{longitude, latitude} \leq 30^\circ \\ \quad \& & \text{longitude} \leq -40^\circ\,, \quad -30^\circ \leq \text{latitude} \end{array}$$

We select periods of 24 hours and calculate the average deposited dose in the specified regions. Periods are rejected when less than 80% of the data is available. For the accepted periods the few missing points are interpolated.

The results are presented in Figure 2. Average daily doses accumulated in the SAA and polar regions are plotted versus time. The upper two panels show SAA data and the lower two represent polar region data. The left and right panels are p–detector and e–detector doses, respectively.

The total average dose rates (dashed lines in Figure 2) measured in the SAA are 75 and 110 mrad/day for p–detector and e–detector, respectively and 5.1 and 150 mrad/day for p–detector and e–detector, respectively in the polar regions.

The SAA doses vary by 50% of the average value. Part of these variations can be accounted for by intrinsic variations due to different passings through the SAA, interpolation of missing data points, and varying orientation of the Mir space station with respect to anisotropic fluxes. We estimate the real variations to be less than 30%. A general increase in the SAA dose towards the end of the observation time can be noted, consistent with approach to solar minimum.

Much larger variations are observed in the polar regions. The e–detector doses vary from approximately 10 mrad/day to 1100 mrad/day. The highest dose rates are encountered during spring and fall, whereas in summer and winter the rates are low. Signs of the enhanced electron population in spring and fall are also seen in the p–detector.

Similar variations of the outer radiation belt population were simultaneously measured with a second REM instrument aboard the UK micro–satellite STRV-1B on a nearly equatorial Geostationary

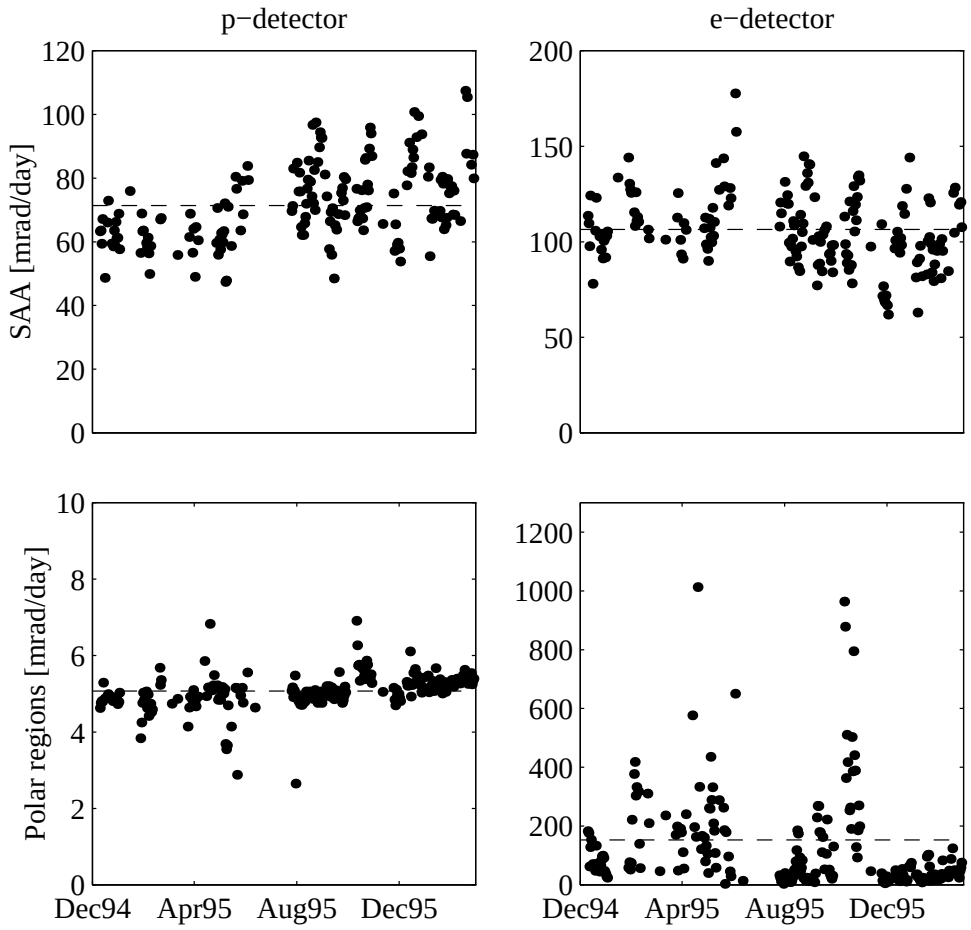

Figure 2: Daily average doses absorbed in the SAA (upper panels) and in the polar regions (lower panels). The left panels are p–detector doses and the right panels, e–detector doses. The horizontal lines show the overall average dose rate. Large variations of the e–detector dose absorbed in the polar regions are observed.

Table 1: Comparison of average daily doses measured with REM and calculated using AP–8 MIN/MAX and AE–8 MIN/MAX radiation models. Values given in brackets are REM minimum/maximum values.

	Average daily doses [mrad]					
	p–detector			e–detector		
	AP–8 / AE–8			AP–8 / AE–8		
	MIN	MAX	REM	MIN	MAX	REM
SAA	50	25	75	90	34	110
			(45 - 110)			(60 - 170)
polar regions	3.0	5.6	5.1	450	1200	150
			(3.6 - 7.0)			(10 - 1100)

Transfer Orbit (GTO) (Bühler *et al.*, 1996). During 1995 the near earth space environment was mainly driven by recurrent fast solar wind streams, which periodically compressed the earth's magnetosphere and caused large variations of energetic trapped particle fluxes in the outer belt. The particle fluxes measured on the nearly equatorial orbit also show a semiannual modulation.

Comparison with NASA AP–8/AE–8 radiation models

AP–8 (Sawyer and Vette, 1976) and AE–8 (Vette, 1991) are radiation models frequently used to estimate expected dose rates for space applications. The models are based on data from the 1960's and 1970's. Two sets of models for solar maximum and minimum conditions exist. Aside this, the models are static. They are thus supposed to describe average values. Comparison of these models with actual data can demonstrate the strong and weak points of the models and the need for updates.

We use the program UNIRAD (Heynderickx *et al.*, 1996) to access the radiation models. UNIRAD allows calculation of omnidirectional trapped particle fluxes for any orbit and their energy deposit at the center of a spherical shell of aluminium as function of its thickness. The standard NASA AP–8 and AE–8 models are accessed via the appropriate geomagnetic field model as described by Heynderickx et al. (1996) and with the correction to the interpolation method by Daly and Evans (1996).

In order to compare model calculations and REM measurements, we need to take the real geometry of the detectors into account. As the dose depth curve of electrons steeply decreases with increasing shielding thickness the contribution of electrons penetrating from outside the entrance cones of $\pm 45°$ to the measured dose rate is assumed to be negligible in both detectors. For electrons, the REM detectors are thus open to 1.84 sr or 14.6% of the entire sphere. To estimate electron REM doses with the radiation models we scale the model values with a factor 0.146. For protons the situation is more difficult since, due to very high energy protons their dose depth curve is expected to be rather flat above 5.9 mm shielding and the contribution of out–of–aperture particles can be important. To approximate the real situation the detector geometry is divided into several segments giving each an average shielding thickness. Then the model dose depth curve, weighted by the viewing angles of the segments is integrated. Contributions from the rear can be neglected as the back of REM is shielded by the space station.

The results of these calculations are listed in table 1 together with the REM measurements.

The REM measurements of the SAA doses in both detectors are larger than the values calculated with the NASA models. REM doses are 25% to 50% higher than AP–8 MIN and higher than AP–8 MAX predictions by a factor 3.
Whereas model predictions for the SAA underestimate the true doses, the AE–8 models give larger doses than measured with REM. Although the maximum REM doses reach the model values, the

average REM dose is lower than the AE–8 MIN and MAX predictions by a factor 3 and 8, respectively. Very similar results have been found with CRRES. In a comparison of the CRRES radiation models (Gussenhoven *et al.*, 1996) with the NASA models it was stated, that for protons with energies above 15 MeV, AP–8 MAX underestimates the CRRES measurements by up to a factor 3 and that the AE–8 MAX model overestimates the CRRES average electron flux by an order of magnitude. This is surprisingly close to what is found with REM, although CRRES has been operational in 1990/91, during solar maximum.

Summary

We have presented LEO energetic particle environment data measured with the REM instrument aboard the Russian Mir space station from November 1994 to February 1996. Two main radiation contributions are present: protons in the SAA and electrons in the polar regions. Depending on the shielding thickness both contributions can be important for the total dose. However, whereas the SAA protons are only little absorbed by the p–detector shielding (3 mm aluminium, 0.75 mm tantalum), the polar region electrons are effectively stopped. Comparing REM doses with AP–8/AE–8 model calculations reveals major differences. The proton models tend to underrate the average REM doses, whereas the electron models largely overestimate the average measured deposited energies.
The SAA REM doses are underestimated by the AP–8 MIN by approximately 25% or by a factor of 3 by AP–8 MAX. The polar regions REM doses have strongly varied during 1995. The peak values reached the AE–8 predictions but the average value was lower by a factor of 3 (AE–8 MIN) to a factor of 8 (AE–8 MAX). Work is continuing on analysing the reasons behind the variablility of the trapped particle populations.

Acknowledgement

We thank L. Maslennikov, N. Shvez, and M. Beliaev for their assistance in preparing the data and D. Heynderickx for providing us with UNIRAD. This study was supported by ESA/ESTEC/WMA Technology Research Contract 11108/94/NL/JG(SC).

References

Bühler, P., Ljungfelt, S., Mchedlishvili, A., Schlumpf, N., Zehnder, A., Adams, L., Daly, E., Nickson, R. (1995), Radiation Environment Monitor, Nucl. Instr. and Meth. in Phys. Res. A, 368, 825

Bühler, P., Desorgher, L., Zehnder, A., Adams, L., Daly (1996), Monitoring of the Radiation Belts with the Radiation Environment Monitor REM, Proceedings of the Radiation Belt Workshop, October 1995, Brussels, in press

Gussenhoven, M.S., Mullen, E.G., Brautigam, D.H. (1996), Improved understanding of the Earth's Radiation Belts from CRRES satellite, IEEE Trans. Nucl. Sci., 43, 2, 353

Heynderickx, D., Kruglanski, M., Lemaire, J., Daly, E.J., and Evans, H.D.R. (1995), The Trapped Radiation Software Package UNIRAD, Belgian Institute for Space Aeronomy, Ringlaan 3, B–1180 Brussels, Belgium

Konradi, A., Badhwar, G.D., and Braby, L.A. (1994), Recent Space Shuttle observations of the South Atlantic Anomaly and the Radiation Belt models, Advances in Space Research, 14, 10, 911

Sawyer, D.M. and Vette, J.I. (1976), AP–8 trapped proton environment for solar maximum and solar minimum, NSSDC WDC–A–R&S 76–06, NASA–GSFC

Vette, J.I. (1991), The AE–8 trapped electron model environment, NSSDC WDC–A–R&S 91–24, NASA–GSFC